JOURNAL OF MATERIALS SCIENCE **34** (1999) 4413–4423

Microstructural characterisation of a glass and a glass-ceramic obtained from municipal incinerator fly ash

J. MA. RINCÓN, M. ROMERO
The Glass-Ceramics Lab, Inst. E. Torroja de Ciencias de la Construccion, CSIC, 28033 Madrid, Spain

A. R. BOCCACCINI*
Fachgebiet Werkstofftechnik, Technische Universität Ilmenau, PF 100565, D-98684 Ilmenau, Germany
E-mail: aldo.boccaccini@maschinenbau.tu-ilmenau.de

Scanning electron microscopy (SEM), energy-dispersive X-ray (EDX) spectroscopy and X-ray diffraction (XRD) analyses were used to characterise the microstructure and chemical composition of a glass and a glass-ceramic material obtained from incinerator filter fly ash. Although the as-quenched material (vitrified fly ash) was amorphous under the detection limits of XRD, a dispersion of droplets indicating glass-in-glass phase separation was observed. In the glass-ceramic material (crystallised vitrified fly ash), crystals belonging to the pyroxene group and spinels were identified. The microstructure of the glass-ceramic consisted of crystals embedded in an amorphous glassy phase. The crystalline phases contain a higher amount of metallic elements (e.g. Al, Cr, Fe, Ni and Zn and most probably also other heavy metals) than the residual glassy phase. A change of composition of the residual glass phase in the glass-ceramic product, in comparison with the parent glass, is considered to explain, in comparative terms, the higher toxic potential of the glass-ceramic over the glass. The present results demonstrate that for an accurate assessment of the correlation between toxicity, release of hazardous compounds and microstructure, high-resolution characterisation techniques must be employed. In this context, the effect of crystallisation on the chemical durability of the products remains as an important area for further research.

1. Introduction

The significance of municipal solid waste incineration is continuously increasing in countries where the population density is high and the availability of space for land-filling is limited, such as the west-European countries and Japan. In Germany and Switzerland, for example, more than 40% of the unrecycled waste is being incinerated and soon this percentage will increase [1]. Although incineration reduces the volume of the waste by approximately 90%, it leaves considerable amounts of solid residues, such as bottom, boiler and filter fly ashes [2, 3]. Filter ashes are produced at a rate of 25–30 kg per 1000 kg of incinerated waste. They are particularly problematic because they contain significant concentrations of heavy metals (e.g. As, Pb, Sb, Sn, Sr) as well as trace amounts of organic pollutants (e.g. polychlordibenzo-dioxins and -furanes). Due to increasingly stringent environmental regulations, these residues are regarded as hazardous in most countries [1–3]. Therefore, they must be deposited in special landfills equipped with careful control of the effluents. This is a costly and environmentally unsatisfactory solution.

Different options are being developed for the decontamination and/or inertisation of incinerator filter fly ash with the final objective of rendering a product that can be reused or, at least, deposited in standard landfill sites without any risk. These technological alternatives include immobilisation by cement-based techniques [1, 4–6], wet chemical treatments [6] and thermal treatments or vitrification [7–11]. Of these, vitrification is the most promising solution, since by melting the residues at temperatures above 1300 °C, a relatively inert glass is produced: the high temperatures involved in the process lead to the complete destruction of the organic pollutant compounds, and heavy metals can be either incorporated in the glassy product or separated from the residue by evaporation or differential precipitation [7–11]. The inert vitreous product can, in principle, be utilised for urban furniture, landscaping

* Author to whom all correspondence should be addressed.

TABLE I SEM/EDX microanalysis (contents in wt %) of the materials investigated and their different phases (the chemical analysis of the original fly ash is given from Ref. [13])

	FA (As-received fly ash[a])	G (Original glass)	G (Droplets)	G (Matrix)	GC (Glassy phase)	GC (Crystalline phase)	GC (Spinel A)	GC (Spinel B)
Na_2O	3.5	n.a.	n.a.	n.a.	n.a.	n.a.	n.a.	n.a.
MgO	2.4	1.26	1.37	1.12	—	3.65	3.55	4.27
Al_2O_3	17.5	15.77	15.51	15.97	16.71	14.51	23.46	32.28
SiO_2	38.0	38.06	37.91	38.21	45.47	35.16	17.90	3.11
P_2O_5	1.6	2.17	2.30	2.09	1.62	2.31	1.09	—
SO_3	0.2	0.66	0.87	0.72	0.79	0.38	0.27	0.11
Cl_2	—	<[b]	<	<	<	≪	≪	≪
K_2O	1.8	2.35	2.18	2.32	4.41	1.12	0.89	0.14
CaO	21.1	23.97	25.66	24.30	22.87	23.25	9.74	1.20
TiO_2	1.7	2.11	1.93	2.08	1.32	2.97	0.93	0.59
Cr_2O_3	—	0.24	—	—	—	—	5.57	10.70
MnO	0.4	0.19	—	—	0.14	0.23	0.26	0.30
Fe_2O_3	8.0	8.07	7.25	8.25	2.23	12.73	16.63	20.01
NiO	—	—	—	—	0.15	0.15	1.34	2.13
ZnO	3.5	5.14	5.02	4.92	4.28	3.50	18.34	25.17

[a]The original fly ash contains PbO (0.3 wt %) according to the chemical analysis.
[b](< means that a small amount of Cl was detected by EDX; ≪ means a much lower amount of Cl detected).
FA: fly ash; G: Glass; GC: glass-ceramic; n.a.: non assessed.

decoration or for road construction. As a disadvantage, vitrification is an energy-intensive process involving relatively high costs. Therefore, its use can only be fully justified if high-quality products with optimised properties can be fabricated, which can thus compete with current materials, for example for building, architectural or insulation applications. The most effective way to improve the properties of the vitrified products without major alterations to the process itself is the induction of a controlled crystallisation, i.e. by forming a glass-ceramic.

In previous reports the possibility of obtaining glass-ceramic materials from vitrified fly ash was demonstrated [12, 13]. The mechanical properties and toxic potential of the glass-ceramics were also determined [14]. However, the crystalline structure of the material was not studied in-depth. A detailed knowledge of the crystalline phases present, their chemical composition and microstructural arrangement is, however, necessary in order to be able to assess quantitatively the correlation between microstructure, mechanical properties and chemical durability of the material and, thus, to optimise the products. In our previous investigation it was found, for example, that crystallisation of the vitrified fly ash product, while being beneficial in terms of mechanical and other physical properties, may increase the toxic potential of the vitrified residue [14]. In the present study a detailed characterisation of the microstructure of the vitrified fly ash product and of the glass-ceramic obtained from it has been conducted. Standard characterisation techniques including scanning electron microscopy (SEM) coupled with quantitative elemental analyses by energy-dispersive X-ray (EDX) spectroscopy and X-ray diffraction (XRD) analyses were used. The results of the microstructure characterisation were analysed with the aim of providing an explanation for the different toxic behaviour of the glass and glass- ceramic products that was measured in the previous study [14].

2. Experimental

The starting glass was obtained by melting fly ash from a municipal incinerator situated in Westfalen (Germany). The fly ash chemical composition is shown in Table I. In addition to the oxides listed, traces of Cl, Sn, Sb, Cd, Ba, As, Sr, Zr, Pb and Mo were also present. The preparation of glasses and glass-ceramics from these particular fly ash was reported in detail in previous studies [12, 13]. Therefore, only a brief description is given here. Batches of the as-received fly ash, placed in alumina crucibles, were heat-treated at 600 °C for 2 h in air, followed by melting in an laboratory furnace at 1300 °C for 2 h. No additives, fluxes or nucleating agents were added. The glass was quenched in air at room temperature. A shiny black-colour glass was thus obtained. The density of this glass, obtained by the Archimedes technique, was 2.80 g/cm^3 [13]. Specimens suitable for microscopic observation were prepared from the as-quenched glass samples. Glass-ceramic samples were obtained by subjecting a sufficient number of specimens to a crystallisation heat-treatment, as follows: the samples were heat-treated at a rate of 10 °C/min to 880 °C, thereafter the samples were hold at this temperature for 4 h and subsequently the temperature was increased to 950 °C at a rate of 5 °C/min. The samples were kept at this temperature for 10 h. At the end, the crystallised samples became amber-brown coloured. During crystallisation formation of macro-porosity did not occur. The density of the crystallised samples, as measured by the Archimedes technique, was 2.89 g/cm^3 [13]. As-quenched and crystallised glasses were ground and milled to produce powders of average particle size <63 μm suitable for

X-ray diffraction (XRD) analysis (Siemens, CuK_α radiation). Scanning electron microscopy (SEM) coupled with energy-dispersive X-ray (EDX) spectroscopy (Jeol JSM-U3, 20 kV acceleration voltage) was used to examine the microstructure and composition of as-quenched glass and glass-ceramic samples on both fracture and polished surfaces. Samples were fractured in a mortar especially designed to obtain fresh fracture surfaces of brittle materials in flexion [15]. The surfaces were etched with a 2% HF solution during 15 s in order to reveal the phases present both in the glass (glass phase separation) and in the glass-ceramic (crystalline phases). After the chemical etching the samples were washed several times using distilled water and alcohol in an ultrasonic bath. This was necessary to remove residuals of HF and external particles adhered to the surfaces. Polished sections were also prepared to a 1 μm finish for SEM/EDX observations by standard grinding and polishing procedures using SiC paper and diamond paste. Polished samples were also etched using solution of 2% HF.

3. Results and discussion

3.1. Vitrified fly ash (amorphous glass)

The as-quenched vitrified fly ash exhibited no signs of crystallisation on the most part of the fracture surface, as determined by SEM observations. The XRD pattern of this material showed the typical halo of amorphous glasses, as reported elsewhere [13], thus confirming the lack of crystallisation, at least under the limits of detection of XRD (crystallinity above $\sim$2 wt% should be detectable by XRD). However, the material exhibited an heterogeneous microstructure due to the existence of numerous droplets of liquid-in-liquid phase separation, as shown in Fig. 1a and b. Dispersion of droplets representing areas of liquid-liquid insolubility is a usual phenomenon in several glasses [16]. In particular, and relevant for this study as discussed below, extensive glass-in-glass separation similar to that exhibited by the present glasses, has been observed in basalt glasses formulated for the immobilisation of nuclear waste [17]. The size of the dispersed tiny droplets was about 0.5 μm and they exhibited a marked white contrast in the SEM, which may indicate an enrichment of heavy metals. Some agglomerations of droplets forming clusters were also observed (Fig. 1b). SEM observations done on polished and etched surfaces confirm the presence of these insolubility droplets. EDX spot analyses (spatial resolution of the order of 0.5 μm) revealed that there are not significant differences in the composition of the phases (i.e. droplets and matrix). The respective quantitative analysis is presented in Table I. A more detailed analysis of the data in Table I must take into consideration the interference of the X-ray diffraction lines of some elements, which could affect the data shown. Thus, for example, the diffraction lines NaK_α and ZnL_α present a strong overlapping, meaning that the indicated ZnO content may include the content of Na_2O also. The same occurs with the lines SK_α and PbM_α , so that the indicated SO_3 content includes also the PbO content in this glass. It must be also pointed out that although the spectra showed a peak corresponding to the element Cl, this was not quantified because the state in which this element is present is not known, i.e. if it is present as a gaseous occlusion or forming part of the vitreous structure. This aspect is relevant for the present vitrified product, since the starting fly ash contains non-specified amounts of organic compounds of Cl. If it could be demonstrated that this element can be entrapped, at least partially, in the vitreous structure, a significant step towards the full inertization of the fly ash via vitrification would have been done. Moreover, the presence of Cl could have a profound effect on the crystallisation behaviour of the vitrified fly ash.

Detailed SEM observations of the fracture surfaces of the vitrified fly ash product reveal the presence of microporosity and the development of incipient crystallisation at the edge of the samples, as shown in Fig. 2a and b. Microporosity may develop as the result of gases entrapped in the glass. These gases may originate in the Cl-containing organic compounds present in the starting fly ash. The crystals observed, which are present in a very low proportion, and therefore are not detected by XRD, are of two types:

(1) Equiaxed polyhedral crystals of about 5 μm size, which showed a high level of electronic emission under the SEM and are possibly spinels containing significant amounts of heavy metals, and

(2) Elongated prismatic crystals of hexagonal cross section of about 10 μm length and 5 μm thickness, which are possibly crystals belonging to the pyroxenes group, as discussed below.

3.2. Crystallised vitrified fly ash (glass-ceramic)

Fig. 3 shows SEM images of different areas on the fracture surface of a sample after the crystallisation heat-treatment. At low magnifications (Fig. 3a), it is possible to see a partially crystallised "shell" having a thickness of about 35 μm. This crystallisation zone does not exhibit an oriented microstructure, as it has been observed in other glass-ceramics [18]. From this "shell", it is possible to see a partially crystallised area, where both elongated and equiaxed crystals are presented, having average size of approximately 5 and 10 μm, respectively (Fig. 3b). The interior of the material shows a high degree of crystallisation, characterised by a network of interlocked elongated crystals between which smaller, equiaxed crystals are situated (Fig. 3c). By SEM observation of polished surfaces of the material, as shown in Fig. 4, the crystalline phases present can be better visualised and distinguished. Particularly using backscattered electrons, a very good contrast between the crystalline phases and the remaining amorphous matrix can be achieved and so the morphology of the crystals can be studied. Thus, in a low-magnification image as shown in Fig. 4, the following features are distinguished:

(a) Polygonal, equiaxed crystals with a very bright contrast, and showing a very dispersed distribution,

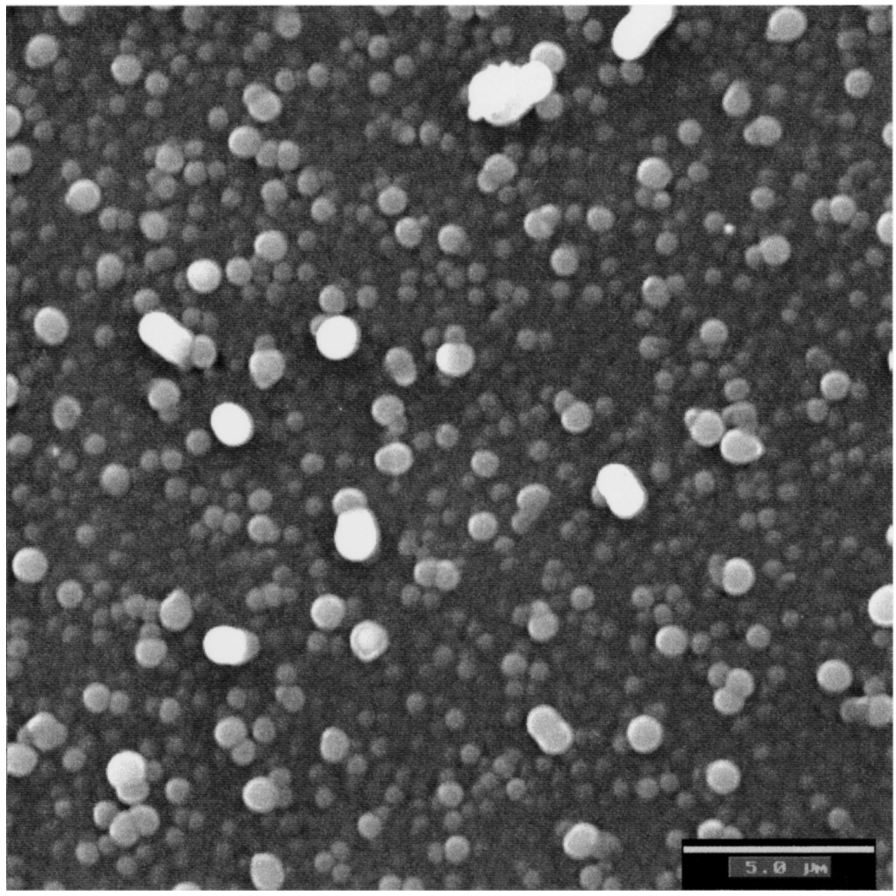

(a)

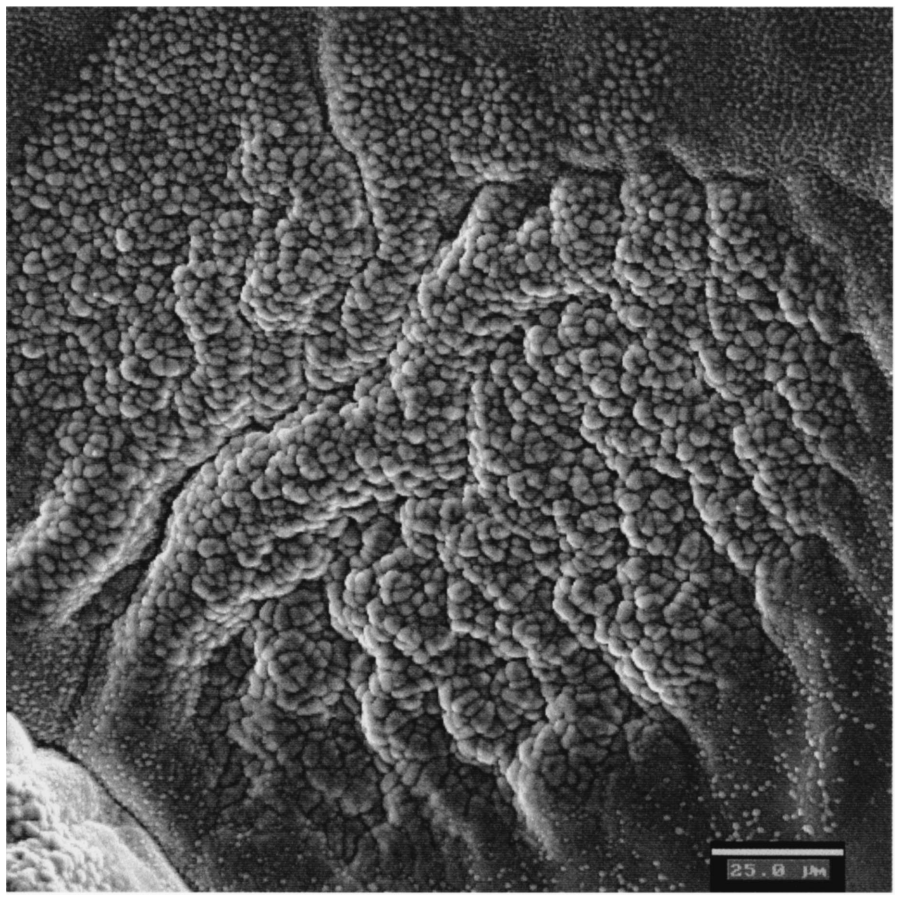

(b)

Figure 1 SEM micrographs of the fracture surface of the as-quenched glass (vitrified fly ash) showing: (a) high dispersion of droplets representing glass-in-glass separation, and (b) agglomeration of droplets.

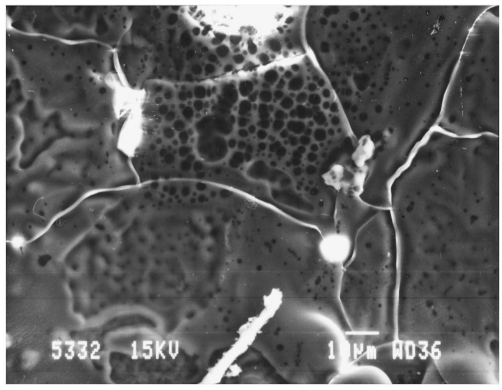

(a)

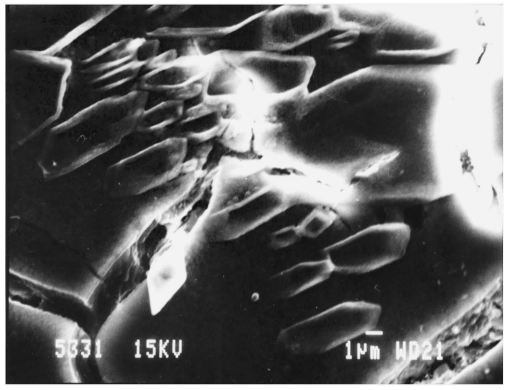

(b)

Figure 2 SEM micrographs of the fracture surface of a glass sample, showing formation of microporosity (a) and incipient crystallisation (b).

(b) Elongated crystals exhibiting a grey contrast and making the most part of the crystalline phase, and

(c) Areas of the amorphous residual glassy phase (matrix), which appears in dark contrast.

Powder XRD diffraction analysis of the sample demonstrates the high level of crystallisation achieved, as shown in Fig. 5. The following crystalline phases were detected, listed in decreasing order of the relative amount found: diopside, anortite (or an anortitic feldspar) and spinel. The crystalline pattern obtained was reproducible and did not depend on the batch of as-received material taken for the experiments. This indicates that the chemical composition of this particular fly ashes was very homogeneous. The relative composition of the different crystalline phases in the glass-ceramic can be assessed by EDX spot analyses on high-magnification SEM images, such as the one shown in Fig. 6. Typical EDX spectra obtained are shown in Fig. 7 and the results of the quantitative analysis are presented in Table I. The data reveal the different chemical composition of the different phases. Thus, for example, although the Al/Si ratio is practically the same for the amorphous and crystalline phase (elongated crystals), the glassy matrix is richer in K, Zn and Cl. This may suggest that Cl could be entrapped as gaseous occlusions in the glass matrix, or that it may be forming part of the silicate glass network. This last hypothesis needs certainly further verification, e.g. by using spectroscopic techniques, but it should be seriously taking into account, particularly considering results in the literature demonstrating the incorporation of cloridic salts in glasses [19–21]. The chemical analysis of the elongated crystalline phase leads to the conclusion that these crystals may correspond to the diopside phase identified by XRD analysis (Fig. 5). Although diopside is a pyroxene crystal of general composition $CaO{\cdot}MgO{\cdot}2SiO_2$, it is well-known that crystals belonging to the pyroxene group, i.e. augite, can be formed by substitutions of the type: $[CaO{\cdot}TiO_2]_x$ $[MgO{\cdot}FeO{\cdot}ZnO]_{1-x}$ $[Al_2O_3{\cdot}Fe_2O_3]_y{\cdot}2SiO_2$. Thus, in the present glass-ceramics, the presence of Fe, Mg, Ca, Zn and Al in the elongated crystals (see Fig. 7b) suggests that these are in fact pyroxenes of the type augite, similar to those formed in crystallised basalt glasses [17, 22], and in model glasses formulated to simulate the composition of vitrified fly ash [21]. This type of pyroxene crystals has been also observed in crystallised glasses obtained from other industrial waste rich in Fe, such as fly-ash from thermal power stations [23] and goethite industrial waste [24, 25]. Besides the uncertainty concerning the state of the element Cl in this material, as mentioned above, also the location of P remains an open question. In particular, it would be interesting to further investigate how this element is incorporated in the crystalline structure of the pyroxenes, since the EDX analyses (Table I) revealed that these crystals contain a higher amount of P than the residual glassy phase. Moreover, the exact chemical composition of the pyroxene crystals can not be further determined using SEM/EDX due to the fine scale of the crystals and the limited spatial resolution of the technique (of the order of 1 μm). In this context, investigations using transmission electron microscopy (TEM) images and quantitative EDX are in progress to gain a more detailed assessment of the exact composition and structure of the pyroxene phase present in these glass-ceramics. The analysis by SEM/EDX of the bright polygonal crystals (Fig. 7c and d and Table I) showed the existence of at least two different (cubic) spinel phases, which will be called spinel A and B. In these phases a high concentration of the metallic elements Fe, Cr, Ni and Zn was found, which are thought to be entrapped in this type of cubic lattice. In spinel B, there is a higher concentration of Ca and Ti, which may suggest the existence of a sphene phase in solid solution with the spinel. Further characterisation of these crystalline phases will need the use of higher resolution techniques including TEM and electron diffraction analyses.

The assessment of the crystallisation kinetics and the accurate identification of crystalline phases and of their chemical composition have been reported to be difficult tasks in this kind of glass-ceramics obtained from vitrified incinerator fly ash [7, 12]. Nevertheless, the present observations and XRD data may help to determine the crystallisation mechanism active in these materials. Thus, Figs 4 and 6 reveal that there is a preferred orientation of the pyroxene crystals with respect to the faces of the cubic crystals of spinel. Most of the elongated crystals have one of their edges in contact with the spinel crystals and are situated perpendicularly to

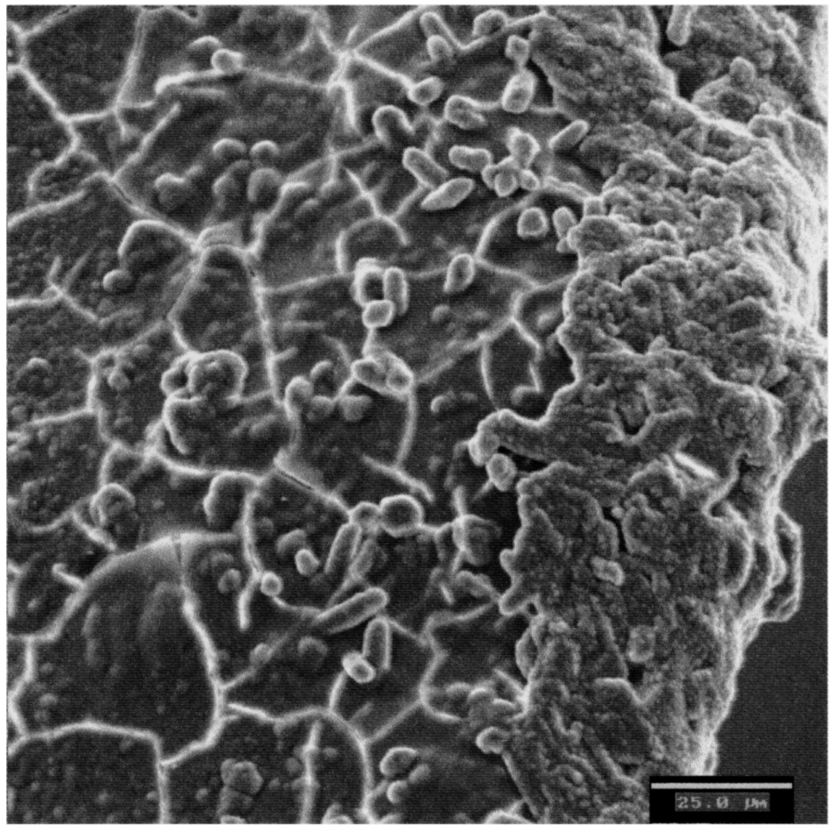

(a)

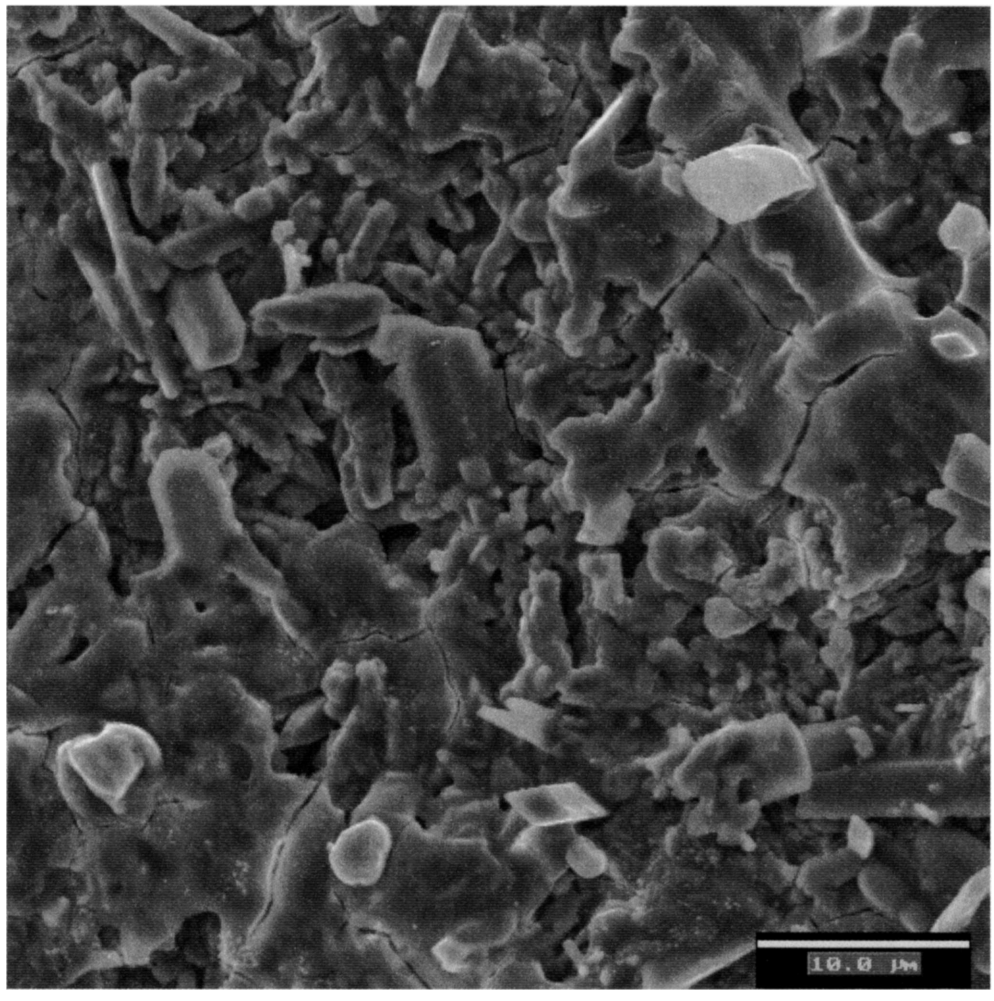

(b)

Figure 3 SEM micrograph of the fracture surface of glass-ceramic sample: (a) low magnification image showing crystallisation "shell", (b) partly crystallised area exhibiting both elongated and equiaxed crystals, (c) highly crystallised area, showing a network of interlocked elongated crystals and smaller equiaxed crystals. (*Continued*)

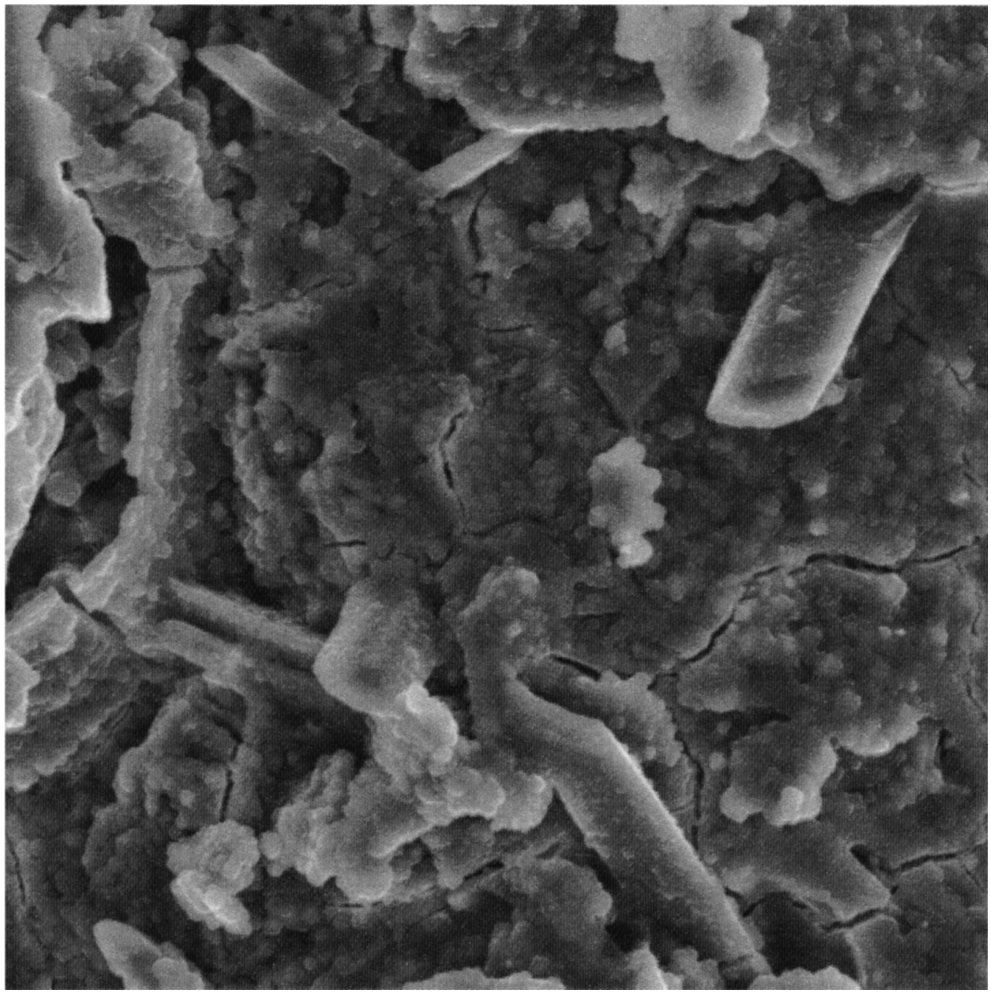

(c)

Figure 3 (*Continued*).

Figure 4 Low-magnification SEM image of a polished surface of a glass-ceramic sample. The microstructure consists of elongated and equiaxed crystals dispersed in an amorphous glassy matrix.

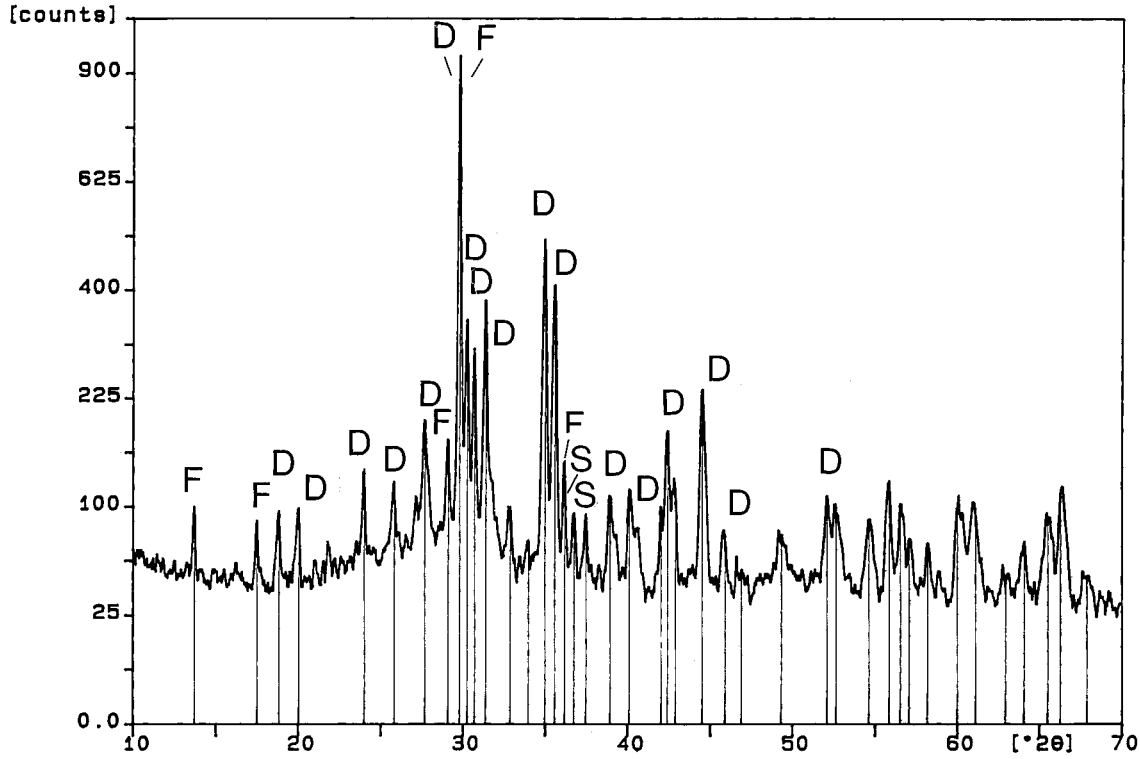

Figure 5 XRD pattern of the glass-ceramic material showing high level of crystallisation. The following crystalline phases are identified: pyroxenes, e.g. diopside (D), anorthitic feldspar (F), spinel (S).

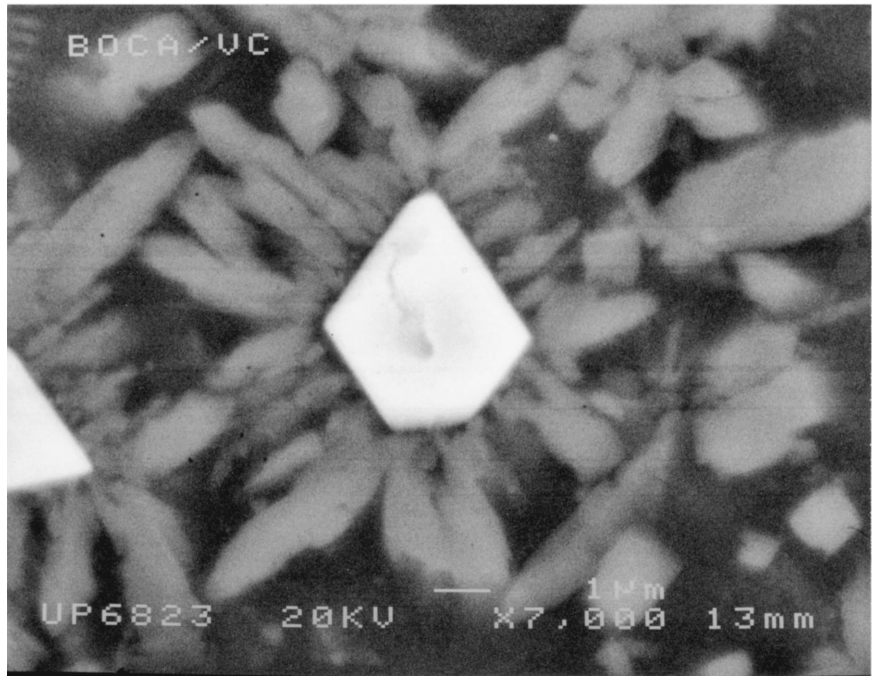

Figure 6 High-magnification SEM image of the polished surface of a glass-ceramic sample showing details of the crystalline microstructure. The following features are distinguished: (i) a polygonal, equiaxed crystal with a very bright contrast (spinel), (ii) elongated crystals exhibiting a grey contrast (pyroxene) and (iii) an amorphous residual glassy phase (matrix), which appears in dark contrast.

the faces of this cubic phase. Therefore, a mechanism for the crystallisation may be suggested, considering the epitaxial growth of the pyroxene crystals from the spinel phase, which being the phase that forms more quickly, would then provide heterogeneous nucleation sites for the further crystallisation progress.

3.3. Crystallisation and toxic potential of the products

The microstructural analysis presented in the previous sections may be used to provide a first (qualitative) explanation for the toxic behaviour of the glass and glass-ceramic materials. In a previous

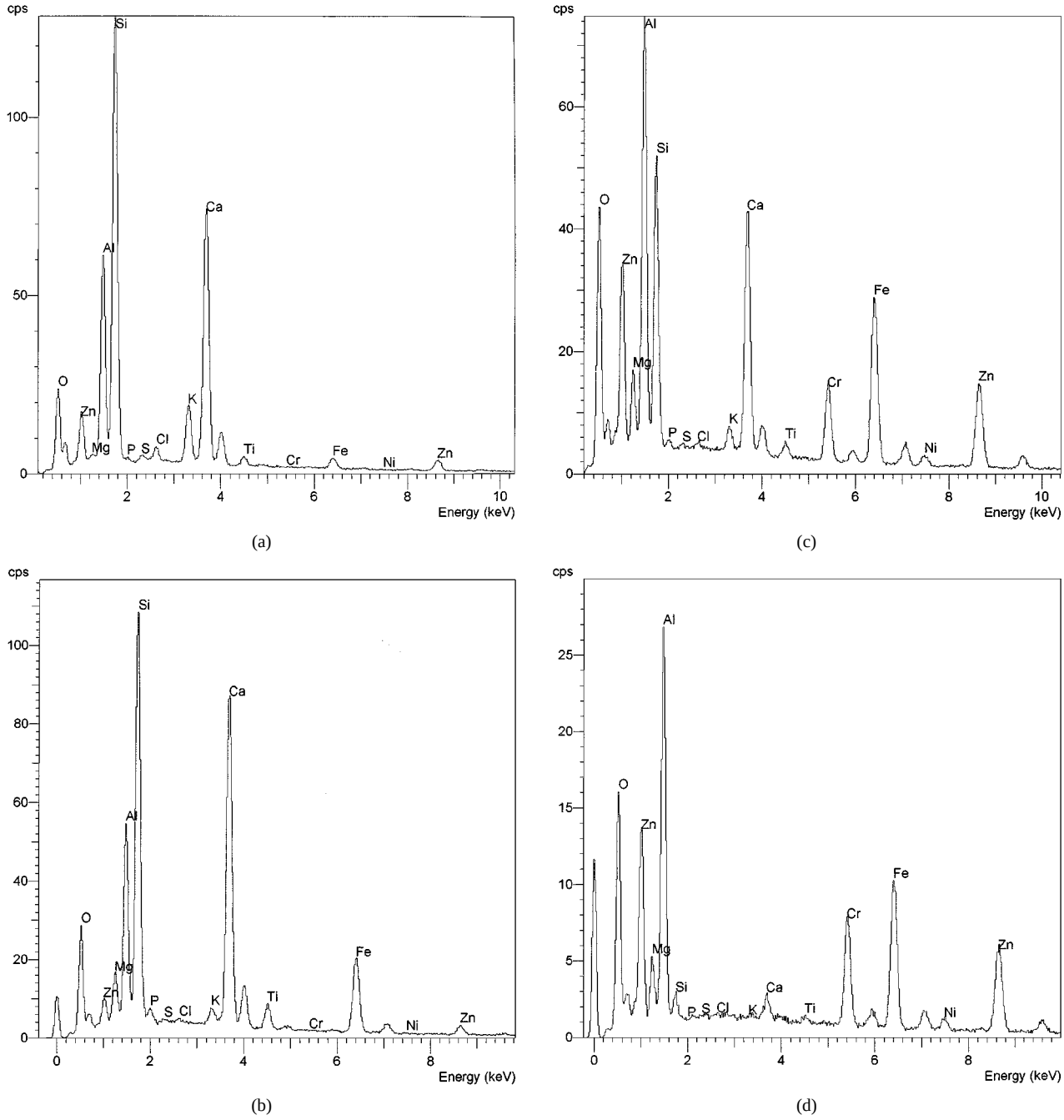

Figure 7 Typical EDX spectra obtained for the different phases in the glass-ceramic sample (see also Fig. 6): (a) glass matrix, (b) crystalline phase, elongated crystals, (c) crystalline phase, equiaxed crystals (spinel A), and (d) crystalline phase, equiaxed crystals (spinel B).

investigation [14], the toxic potential of the materials was assessed by cell culture tests. By measuring the cell activity after contact with extracts from the samples, it was shown that the toxic potential of the glass-ceramic material was higher than that of the as-quenched glass. The results of those toxicity measurements are summarised in Fig. 8, where toxicity, as quantified by the cell activity of a cell culture medium treated by extracts of the samples [26], has been plotted for different concentration of extraction media. The toxicity data were normalised to the values determined for a petri dish glass, which was assumed to be non-toxic. The results shown in Fig. 8 indicate that the release of substances that inhibit cell activity, for example heavy metals, was more pronounced in the crystallised samples. Since both glass and glass-ceramic specimens were similarly dense (with negligible microporosity), a possible effect of porosity on the different toxic potential of the materials can be ruled out. Assuming that most heavy metals are concentrated in the crystalline phases, as the SEM/EDX analyses of the present investigation suggest, the increase of toxicity of the glass-ceramic could be simply explained on the basis of a poorer leaching resistance of these crystalline phases in comparison with that of the parent glass matrix. Results in the literature disagree on the influence of crystallisation on the leaching resistance of heavy metal containing glasses. For example, in glasses prepared from steel making precipitator dusts and silica [27], crystallisation was shown to affect negatively the leaching behaviour, whereas for glass-ceramics prepared from basalt glasses [17], goethite waste [24], hazardous waste incinerator residuals [28] and lead-containing waste glass [29], crystallisation

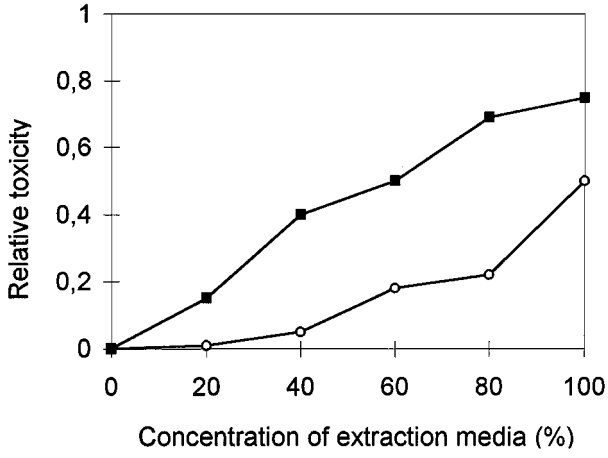

Figure 8 Relative toxicity of the materials investigated, according to the results of a previous study [14] using the cell culture tests: (■) glass-ceramic, (○) as-quenched glass. The data were normalised with respect to the toxicity of petri dish glass, whose toxicity was assumed to be nil.

resulted in a higher chemical durability. In yet other observations on simulated nuclear waste glasses, crystallisation was found to have no effect on the leaching behaviour of the samples [30]. It is interesting to note that the microstructure of the present glass-ceramics, exhibiting crystalline phases embedded in a glassy matrix, is exactly opposite to that of the crystallised lead-containing glasses developed by Dwivedi *et al.* [29]. In those samples lead-rich glassy islands were embedded in a crystalline matrix with low lead concentration. Thus, during leaching tests, most of the surface exposed to the acidic extraction fluid was a lead-deficient crystalline matrix while most part of the lead was immobilised in glassy pockets, resulting in less lead being extracted from the glass-ceramic. In the present glass-ceramic, according to the results of the EDX analyses (Table I), the heavy metals are most probably concentrated in the crystalline phases, which may be expected to have a lower chemical resistance than the amorphous glass matrix, thus leading to the poorer chemical durability of the glass-ceramic. In this context, the present results contradict the claim of an earlier waste management approach [31], in which the heterogeneous dispersion of hazardous element-containing particles in a glass matrix (i.e. forming a composite material), was proposed to lead to a good chemical durability of the products. The present results show that the encapsulation of crystalline particles containing heavy metals in a glass matrix does not guarantee *per se* a low leachability of the products.

Assuming that the toxic potential of the materials (Fig. 8) correlates directly with their chemical durability, the present results may be rationalised on the basis of the hypothesis of Chick *et al.* [17] for basalt glass-ceramics. The microstructure of the material investigated by Chick *et al.* resembles that of our glass-ceramics, i.e. they observed the presence of crystalline phases, including pyroxenes, embedded in a glassy matrix. They showed that the durability of the continuous glass phase controlled the leaching behaviour in both the parent glass and the glass-ceramic, and explained the higher chemical durability of their glass-ceramic materials by considering the change of composition of the glass residual phase. They speculated that the increased chemical durability of the glass-ceramic was due to the removal of alkaline-earth elements (e.g. Ca, Mg) from the glass matrix phase to form the pyroxene phase, in particular augite. With less concentration of alkaline-earth elements, the glass network should be more resistant to chemical attack. The authors also noted that in their glasses, the effect of removal of alkaline-earth elements from the glass matrix phase would overcome the observed enrichment of this phase in Na. This element is expected to affect negatively the chemical durability of the products. In our glass-ceramics, a depletion of the elements Ca and Mg in the glass phase was detected (see Table I). However, this is not as pronounced as that shown to occur in the basalt glass-ceramics of Chick *et al.* [17]. In particular, in that investigation, the concentration of Ca in the glass phase of the glass-ceramic was shown to be less than 50% of that in the as-quenched glass [17]. In our material this difference was only of 8% (Table I). Moreover, since the concentration of Na could not be quantified with the SEM/EDX technique used (due to the overlapping of the K_α line of Na and L_α line of Zn), the possible change of Na concentration in the glassy phase of the glass-ceramic can not be ruled out nor confirmed, this being an interesting topic of research for future studies. Thus, analysing the present data and literature results, seems that there is no universal explanation for the effect of crystallisation on leaching behaviour, and that each glass-ceramic system must be analysed separately. For the present glass-ceramics, further microstructure and chemical analyses utilising measurement techniques of higher resolution are required in order to obtain a more clear view of the relationship between crystallisation and chemical durability. In particular, the distribution and relative concentration of the elements Cl, P, Na and of the heavy metals in the different phases must be assessed. The potential hazardous effect of these materials should be further analysed by conducting chemical durability tests (e.g. Soxhlet, "Swiss" [21] or DEV-S4 tests [32]), in addition to the toxicity tests described elsewhere [14].

4. Conclusions

The microstructure of a glass and a glass-ceramic material obtained from incinerator filter fly ash was investigated. The as-quenched material (vitrified fly ash) was amorphous under the detection limits of XRD. Tiny droplets of glass-in-glass phase separation were observed, however. In the glass-ceramic material (crystallised vitrified fly ash), crystals belonging to the pyroxene group and spinels were identified. These crystals are embedded in an amorphous glassy phase. The particular arrangement of the crystalline phases lend to the conclusion that the pyroxene crystals may have grown epithaxially from the faces of the cubic spinels. The crystalline phases contain a higher amount of metallic elements (e.g. Al, Cr, Fe, Ni and Zn and heavy metals) than the residual glassy phase. Following an explanation advanced by Chick *et al.* [17], the change

of composition of the glass phase in the glass-ceramic product, in comparison with the parent glass, seems to be the key factor explaining its higher toxic potential, as found in a previous study [14]. The existence of Cl in the glass and glass-ceramic was confirmed, but little is known on the way it is incorporated in the glassy and crystalline phases. The exact correlation between toxicity, release of hazardous compounds and microstructure of these materials must be further investigated. This will help to answer the open remaining questions concerning the chemical durability and toxic potential of the products, and how these are changed by the crystallisation. Only after these questions have been fully addressed and clarified, it will be possible to consider realistically the materials for the envisaged technical applications.

Acknowledgements

The authors acknowledge the experimental possibilities to carry out this investigation offered by the Laboratory of Electron Microscopy (Inst. Nacional de Técnica Aeroespacial), Torrejón de Ardoz (Madrid) and by the Electron Microscopy Service, (Polytechnic University of Valencia).

Part of this work was carried out with financial support from the program "acclones Inteprades," funded by DAAD (Bonn) and Ministerio de Educación y Cultura (Madrid).

References

1. O. HJELMAR, *J. Hazardous Mat.* **47** (1996) 345–368.
2. R. DERIE, *Waste Management* **16** (1996) 711–716.
3. P. T. WILLIAMS, in "Waste Incineration and the Environment, Issues in Environmental Science and Technology," edited by R. E. Hester and R. M. Harrison (Royal Society of Chemistry, 1994) pp. 27–52.
4. G. C. C. YANG and S.-Y. CHEN, *J. Hazardous Materials* **39** (1994) 317–333.
5. M. T. ALI and W. F. CHANG, *ACI Materials Journal* **91** (1994) 256–263.
6. O. BARIN, *Wiss. und Umwelt* **3/4** (1991) 159–167.
7. R. GUTMAN, *Glass Sci. Technol.* **69** (1996) 285–299.
8. R. MERGLER, *Glas-Ingenieur* **6** (1993) 83–88.
9. M. KRAUß, *Glastech. Ber. Glass Sci. Technol.* **70** (1997) 375–381.
10. D. DE LABARRE, *Verre* **3** (1997) 33–39.
11. D. F. BICKFORD and R. SCHUMACHER, *Ceram. Eng. Sci. Proc.* **18** (1995) 1–10.
12. A. R. BOCCACCINI, M. KOPF and G. ONDRACEK, *Z. Angewandt. Umweltforschung* **7** (1994) 357–367.
13. A. R. BOCCACCINI, M. KOPF and W. STUMPFE, *Ceram. Int.* **21** (1995) 231–235.
14. A. R. BOCCACCINI, M. PETITMERMET and E. WINTERMANTEL, *Ceram. Bull.* **76** (11) (1997) 75–78.
15. P. CALLEJAS, Obtención, Microestructura y Propiedades de Materiales Vitrocerámicos con Efecto Aventuvina, Ed. Univ. Autónoma de Madrid (1988) p. 46.
16. H. RAWSON, "Properties and Applications of Glasses" (Elsevier, Amsterdam, 1980) p. 22.
17. L. A. CHICK, R. O. LOKKEN and L. E. THOMAS, *Ceram. Bull.* **62** (1983) 505–516.
18. J. MA. RICON and R. CAPEL, *Ceram. Int.* **11** (1985) 97–102.
19. C. HIRIYAMA and F. E. CAMP, *Glass Technol.* **10** (1969) 123–127.
20. J. MA. RINCON and H. MARQUEZ, "Electron Microscopy," Vol. 2 (EUREM 92, Granada, Spain, 1992) pp. 455–456.
21. A. KIPKA, B. LUCKSCHEITER and W. LUTZE, *Glastech. Ber.* **66** (1993) 215–220.
22. J. MA. RINCÓN and M. ROMERO, *Mat. de Construccion* **46** (1996) 91–106.
23. L. BARBIERI, T. MANFREDINI, I. QUERALT, J. MA. RINCON and M. ROMERO, *Glass Technol.* **38** (1997) 165–170.
24. M. PELINO, C. CANTALINI and J. MA. RINCÓN, *J. Mater. Sci.* **32** (1997) 4655–4660.
25. M. ROMERO and J. MA. RINCÓN *J. Europ. Ceram. Soc.* **18** (1998) 153–160.
26. M. PETITMERMET, A. FAVRE, B. SHAH, U. RÖSLER, J. MAYER and E. WINTERMANTEL, in "Monitoring and Verification of Bioremediation," edited by R. E. Hinchee, G. S. Douglas and S. K. Ong (Battelle Press, Columbus, 1995) pp. 223–232.
27. T. R. MEADOWCROFT, *Mat. Trans. JIM* **37** (1996) 532–539.
28. S. D. KNOWLES and D. A. BROSNAN, *Canadian Ceramics Quarterly J. Canad. Ceram. Soc.* **64** (1995) 231–234.
29. A. DWIVEDI, Y. BERTA and R. SPEYER, *J. Mater. Sci.* **29** (1994) 2304–2308.
30. M. A. AUDERO, A. M. BEVILACQUA, N. B. M. BERNASCONI, D. O. RUSSO and M. E. STERBA, *J. Nuc. Mat.* **223** (1995) 151–156.
31. A. R. BOCCACCINI, J. JANCZAK, D. M. R. TAPLIN and M. KÖPF, *Environmental Technology* **17** (1996) 1193–1203.
32. L. DEPMEIER, U. TOMSCHI and G. VETTER, *Müll und Abfall* **9** (1997) 528–533.

Received 20 October 1998
and accepted 3 March 1999